Impact of Environmental Variables on the Reduction of Nitric Acid by Proxies for Volatile Organic Compounds Emitted by Motor Vehicles

Leong Y. J.[1,*]; Rutter, A. P.[1,2]; Wong, H. Y.[1,3]; Gutierrez, C. V.[1]; Junaid, M.[1]; Scheuer, E.[4]; Gong, L.[1,5] ; Lewicki, R.[6,7]; Dibb, J. E.[4]; Tittel, F. K.[6]; Griffin, R. J.[1]

[1] Rice University, Civil and Environmental Engineering, 6100 Main Street MS-519, Houston, TX 77005, United States

[2] (Current) Collaborative Sciences Division, S.C. Johnson, Inc., 1525 Howe St., Racine, WI 53403, United States

[3] (Current) Behn Meyer Group Malaysia, 5, Jalan TP2 Sime UEP Industrial Park, Subang Jaya, Selangor, 47600, Malaysia

[4] University of New Hampshire, Earth Systems Research Center, Morse Hall, Durham, NH 03824, United States

[5] (Current) Monitoring and Laboratory Division, California Air Resources Board, 1900 14th Street, Sacramento, CA 95811, United States

[6] Department of Electrical and Computer Engineering, Rice University, 6100 Main Street, MS 366, Houston, TX 77005, United States

[7] (Current) Sentinel Photonics, 45 Wall Street, Princeton, NJ 08540, United States

*Corresponding author: Yu Jun Leong, Email: yu.jun.leong@gmail.com. Phone: (713) 348-3036. Fax: (713) 348-5268.

Abstract

Recent work has identified nitric acid (HNO_3) as a potential precursor of nitrous acid (HONO), which is an important source of oxidants that regulate ozone and particulate pollution. Recent work in our laboratory has indicated that the reduction of HNO_3 to HONO can occur homogeneously in the presence of surrogates for volatile organic compounds (VOCs) emitted by motor vehicles. This study focuses on the impact of environmental variables on the rate of formation of HONO in this process. The observed base case (25.0°C and ~20.0% relative humidity (RH)) HONO formation rate was 0.54 ± 0.09 ppb hr^{-1}, values comparable to enhancements observed in HONO during morning rush hour in Houston, TX. The rate was enhanced at lower temperatures of ~20.0°C, but the rate remained statistically similar (1σ) for experiments conducted at temperatures of 25°C, 30°C, and 35°C. The assumption that multiple reactive components of the VOC mixture react with HNO_3 is supported by this observation, and the relative importance of each reactive species in the reaction may vary with temperature. The enhanced

rate at lower temperatures could make the proposed reaction mechanism more important at night. The formation rate of HONO does not change substantially when initial HNO_3 concentration is varied between 400 and 4 600 ppt, suggesting that the concentration of reactive VOCs was the limiting factor. The reduction of HNO_3 to HONO appears not to occur heterogeneously on the aerosol surfaces tested. The presence of ~120 ppb of ammonia has no observable impact on the reaction. However, it is likely that UV irradiation (λ = 350 nm) decreases the formation rate of HONO either by consuming the reactive VOCs involved or by directly interfering with the reaction. The "renoxification" of less reactive HNO_3 to more reactive HONO has significant implications for daytime ozone and particulate pollution.

Keywords

Nitrous acid; nitric acid; volatile organic compounds; flow tube; reduction-oxidation

1. Introduction

Nitrous acid (HONO) is an important trace gas in the regional and global troposphere. It can have significant air quality implications due to its photolysis, yielding nitrogen oxide (NO) and the hydroxyl radical (OH) (Atkinson, 2000):

$$HONO + h\nu \rightarrow OH + NO \qquad \text{(R1)}$$

The OH radical serves as a strong oxidant in the atmosphere and is partly responsible for the chemical processes that lead to the formation of tropospheric ozone (O_3) (Finlayson-Pitts and Pitts, 1997) and secondary particulate matter (PM) (Kanakidou et al., 2005). With nitrogen dioxide (NO_2), NO contributes to total nitrogen oxide (NO_x) levels. The potential of a regional air mass to produce O_3 depends strongly on the relative abundance of volatile organic compounds (VOCs) and NO_x. Because HONO influences NO_x levels, O_3 pollution levels are highly sensitive to HONO levels under particular conditions (Harris et al., 1982; Lei et al., 2004; Carter and Seinfeld, 2012). Harris et al. (1982) observed increases in O_3 dosages up to a factor of 3 when 10 ppb of HONO is included in model simulations. Using a three-dimensional chemical transport model, Lei et al. (2004) estimated up to 12 ppb enhancements in O_3 levels in Houston, TX, due to a proposed heterogeneous source of HONO. Zero-dimensional model simulations of O_3 formation episodes in the Upper Green River Basin in Wyoming during winter predicted strong O_3 sensitivity to HONO levels (Carter and Seinfeld, 2012).

Nitrous acid mixing ratios observed at various urban sites range from 0.4 to 8.0 ppb at night and 100 to 300 ppt during the day (Harris et al., 1982; Harrison et al., 1996; Kleffmann, 2007; Wong et al., 2011; Indarto, 2012), while concentrations at rural sites were 10 to 200 ppt (Cape et al., 1992; Zhou et al., 2002; Zhou et al., 2011). A known source of HONO during daytime in polluted environments is the reaction between OH and NO (Atkinson, 2000):

$$OH + NO + M \rightarrow HONO + M \qquad \text{(R2)}$$

Nitrous acid builds up overnight from (R2) (when OH and NO persist without sunlight) and other sources and photolyzes in the morning, causing a spike in OH and NO_x, resulting in accelerated O_3 production (Harris et al., 1982). Nitrous acid sources other than (R2) are thus highly important due to their potential to contribute to both daytime and nighttime HONO levels. Modeling studies have concluded that HONO sources are still missing from current hydrogen oxide (HO_x) and NO_x chemistry models, resulting in the underprediction of HONO or O_3 levels (Grannas et al., 2007; Wong et al., 2011; Carter and Seinfeld, 2012).

A number of recent studies have documented possible sources of HONO from HNO_3 or NO_2. Kleffmann (2007) proposed several formation mechanisms: heterogeneously on surfaces treated with HNO_3, from the reduction of NO_2 on photosensitized organic surfaces, and via photolysis of ortho-substituted nitroaromatics. Similarly, photolytic conversion of NO_2 to HONO on polycyclic aromatic hydrocarbon films was observed by Cazoir et al. (2014). Grannas et al. (2007) summarized several HONO formation mechanisms in a snowpack. In urban New Zealand, Reisinger (2000) observed a good correlation between $HONO/NO_2$ (a metric for the relative abundance of HONO) and aerosol surface density, indicating a heterogeneous HONO source. Nitrous acid forms on the surface of soot particles from NO_2, but the reaction is not considered a major contributor to HONO under typical ambient conditions (Ammann et al., 1998; Kalberer et al., 1999). Kirchstetter et al. (1996) measured vehicular emissions of HONO in the Caldecott Tunnel, but the observed $HONO/NO_2$ ratios were much lower than the nighttime values measured under ambient conditions. In addition, recent airborne measurements coupled with zero-dimensional model simulations inferred a strong gas-phase source within the residual layer with formation rates that scaled with HONO photolysis rates (Li et al., 2014). The authors argued that this unknown source could dominate overall HONO production in the planetary boundary layer, exceeding surface HONO sources. The proposed ultraviolet (UV)-dependent HONO source was likely internal (from the reaction of NO_x and/or HO_x). Liu et al. (2014) proposed a substantial heterogeneous HONO source from the hydrolytic disproportionation of NO_2 on aerosol to help explain missing daytime HONO sources in China. Flow tube studies by VandenBoer et al. (2015) suggested a nighttime soil sink of HONO, leading to daytime acid displacement and release of HONO. A review of the current state of the science for HONO can be found in Spataro and Ianniello (2014).

In September 2006 in Houston, TX, Ziemba et al. (2010) observed HNO_3 depletion concurrent with increases in HONO concentrations and aerosol surface area dominated by a proxy for primary organic aerosol (POA). The authors hypothesized a heterogeneous reaction between HNO_3 and POA to form HONO, which supports the findings from previous studies that document the heterogeneous reduction of HNO_3 (Zhou et al., 2002; Rivera-Figueroa et al., 2003; Zhou et al., 2003; Zhou et al., 2011).

In an effort to better understand the phenomenon observed by Ziemba et al. (2010), Rutter et al. (2014) performed a series of flow tube experiments in which gaseous HNO_3 was observed to be reduced homogeneously to HONO by VOCs representative of those emitted from motor vehicles via the hypothesized reaction:

$$HNO_3 + VOC \rightarrow HONO + VOC_{ox} \qquad \text{(R3)}$$

The reported formation rate of HONO was 0.3 ± 0.1 ppb hr^{-1} under a defined base case of 25.0°C and RH of ~20%. The HONO formation rates decreased with increasing RH. Increased surface area in the flow-tube (Teflon© Raschig rings and/or a surrogate for vehicular POA) had no impact on HONO formation. The experiments described here used a slightly modified and improved version of the flow-tube system of Rutter et al. (2014) to further characterize this HONO formation reaction by varying temperatures and HNO_3 concentrations, irradiating, or adding ammonia (NH_3) or mineral dust surrogates. These experiments are designed to improve our understanding of the importance of the proposed HONO formation reaction under varying ambient conditions and to assess its potential to enhance HONO levels in the atmosphere.

2. Experimental

2.1 General Information

The flow-tube system used in this study is described by Rutter et al. (2014), with improvements and additional instrumentation described below. Briefly, HNO_3 gas and VOCs from a specific blend of vehicle engine oil (Supporting Material, Table S1) were introduced into a quartz flow reactor, which is located in a temperature-controlled chamber. Nitric acid was generated from a permeation device (Dynacal, VICI Metronics, Poulsbo, WA), and engine oil particles along with VOCs were introduced using a TSI 3076 atomizer (Shoreview, MN) with a Teflon® filter in-line when the particles were not desired. A combustion VOC surrogate was not used for this study as the original intent was to use reduced organics from motor oil (Rutter et al., 2014); this avoids possible HONO artifacts from combustion exhaust (Kirchstetter et al., 1996). A recent tunnel study showed that a large portion of vehicular POA is similar in composition with unburned motor oil (Worton et al., 2014). The VOCs used in this study were intended to serve as surrogates for VOCs produced from the volatilization of vehicular POA under ambient conditions. The outflow from the flow-tube was sampled by a refurbished on-line mist chamber-ion chromatograph (MC/IC) system (Rutter et al., 2014) to obtain 10-minute HONO and HNO_3 concentrations. This measurement technique has been tested and characterized extensively (Talbot et al., 1990; Dibb et al., 1994; Dibb et al., 1998; Dibb et al., 2002) and showed good comparison with Differential Optical Absorption Spectroscopy (Stutz et al., 2010). A new quartz flow-tube with dimensions identical to those of the reactor in Rutter et al. (2014) was used and was passivated by a non-reactive halocarbon wax coating to minimize wall reactions. Instrumentation used to measure temperature, RH, and particle number concentration were outlined in Rutter et al. (2014). The instrumentation for measuring NH_3 is described below.

In this study, the base case experiments were conducted at a temperature of 25°C and a RH of ~20% while maintaining a mean HNO_3 concentration of 2.4 ppb and a constant level of VOCs in the flow-tube reactor. For each experiment, the flow-tube reactor was allowed to equilibrate at the desired conditions (concentrations of HNO_3 and VOCs, temperature, RH, and other variables). The formation rates of HONO (f_{HONO}, ppb hr^{-1}) were calculated using the step change in HONO concentrations when VOCs were removed:

$$f_{HONO} = ([HONO]_t - [HONO]_0) / t_{res} \qquad \text{Equation (1)}$$

where $[HONO]_t$ (in ppb) was the average steady-state HONO concentration measured when VOCs were present to react with HNO_3, $[HONO]_0$ was measured after VOCs were removed and only HNO_3 was present, and t_{res} is the average residence time of all gases in the flow-tube (150 s). Detailed descriptions of a typical experiment can be found in Rutter et al. (2014), and all experiments described in this study follow the same procedures except the modifications mentioned below. Additional experimental information is provided in the Supporting Material and Table S2.

Engine oil particles (100 nm, < 150 #/cm^3) were shown in Rutter et al. (2014) to have no effect on the reaction. During several tests, larger concentrations of motor oil particles were injected (up to 1400 #/cm^3) into the mixture of VOCs and HNO_3, and the particles had no observable impact on HONO levels. Therefore, for all experiments presented here motor oil particles were not considered relevant and were excluded by filtering the output from the atomizer upstream of the flow tube reactor. Figure 1 depicts the experimental setup used in this study. A detailed diagram for the delivery of HNO_3 and VOCs can be found in Rutter et al. (2014).

Variations to the base case experiments were achieved by independently varying chamber temperature or HNO_3 concentration or by introducing UV irradiation, NH_3, or mineral dust aerosol surrogate to the system. When a parameter was altered or a new constituent was added, all other base case variables remained unchanged. Apart from HNO_3 and NH_3 experiments discussed in sections 2.3 and 2.4, all experiments in this study were conducted at initial HNO_3 concentrations of ~2-4 ppb for consistency with the experiments of Rutter et al. (2014) and the field measurements of Ziemba et al. (2010).

2.2 Temperature

This study aims to investigate the sensitivity of f_{HONO} to reaction temperature. Because the proposed reduction reaction of HNO_3 by VOCs may involve simultaneous reactions of different reactive VOCs of the engine oil blend, the temperature dependence of the overall formation rate is not expected to follow Arrhenius behavior. Investigation of temperature dependence is achieved by a temperature-controlled environmental test chamber (Espec North America Inc., Hudsonville, MI). The flow-tube and other components were allowed to equilibrate at the desired set-point temperature before an experiment. The measured reactor outflow temperatures were within ~1°C of the set-point chamber temperatures. The temperature range tested here is relevant for the conditions observed in the 2006 Houston field study.

2.3 HNO_3 Concentration

Initial HNO_3 mixing ratios were kept relatively constant in the experiments by Rutter et al. (2014), but minor fluctuations in HNO_3 between experiments were impossible to avoid. Nitric acid concentration was not considered important by Rutter et al. (2014) because the HNO_3 levels were in excess of the estimated 200 - 300 ppt reactive VOCs in the reactor. Here, experiments conducted at different initial concentrations of HNO_3 were used to probe this hypothesis and to investigate potential impacts of HNO_3 levels on the proposed reaction.

The steady-state HNO_3 concentrations in the flow-tube were varied in these experiments by operating the permeation device at different temperatures or by shutting off its supply entirely. Holding other parameters constant, HNO_3 mixing ratios of approximately 4.0 ppb, 1.5 ppb, and 0.4 ppb were achieved. The corresponding experiments are henceforth referred to as high HNO_3, medium HNO_3, and low HNO_3 experiments.

2.4 NH_3

Ammonia reacts with HNO_3 to form ammonium nitrate (NH_4NO_3), which transitions to the particulate phase when specific thermodynamic criteria are met. This reaction is hypothesized as a potential competing reaction and was studied in the flow-tube reactor by the addition of NH_3. Experiments were performed by injecting 118.0 ± 2.0 ppb of gas-phase NH_3 to the flow-tube reactor. A 1-ppm NH_3 cylinder supplied the NH_3 gas stream, which was diluted upon entering the reactor. Ammonia concentrations were monitored using a 10.4-µm external cavity quantum cascade laser that has been well characterized and tested (Gong et al., 2011; Gong et al., 2013). The instrument has a detection limit of 0.7 ppb and an accuracy of 7%, with a maximum time-resolution of 1 s. Because the MC collection efficiencies for HNO_3 and HONO already exceed 95% (Dibb et al., 1994), NH_3 is not expected to cause interferences in HNO_3 and HONO measurements. There was no evidence of artifacts from particulate NH_4NO_3 because the MC/IC sample stream was filtered.

2.5 UV Irradiation

A HONO artifact at a forested field site correlated with UV intensity, possibly due to the photochemical conversion of HNO_3 to HONO on the wall of a glass sampling manifold (Zhou et al., 2002). Laboratory experiments conducted by Zhou et al. (2003) found evidence that photolysis of adsorbed HNO_3 on Pyrex surfaces yields HONO, and Zhou et al. (2011) found a significant HONO daytime source from the photolysis of HNO_3 on forest canopies. These findings emphasize the potential role of UV irradiation in the conversion of HNO_3 to HONO. Despite the observations of Rutter et al. (2014) and Ziemba et al. (2010) that light is not required for the proposed (R3) to proceed, it is hypothesized that UV irradiation may either accelerate (R3) or dampen it by consuming the reactive VOCs involved. Thus, experiments were conducted to test the sensitivity of f_{HONO} to UV irradiation.

Four 4-ft, 40W Sylvania 350BL lights (Osram Sylvania, Danvers, MA) irradiated the flow-tube reactor for one set of experiments. Totaling 160W of output, these tubes were mounted above the reactor and were distributed evenly along the length of the reactor. The reactor and lights were encased in Mylar reflective material to maximize light intensity and to ensure uniform distribution of the artificial light (peak λ = 350 nm). The same type of lights was used in the chamber experiments of Cocker et al. (2001). This wavelength produces maximum NO_2 photolysis rates (Carter et al., 1995) and falls within the UV-A spectrum (320 to 400 nm), which has been reported to photolyze species such HONO (Stutz et al., 2000; Alicke et al., 2002). Thus, the lamps were considered a viable starting point to test for direct interferences on the hypothesized HONO formation reaction.

2.6 Mineral Dust Aerosol Surfaces

Field data collected in Houston during 2006 showed the potential for heterogeneous reduction of HNO_3 into HONO on urban aerosol (Ziemba et al., 2010). However, Rutter et al. (2014) showed that the HONO formation reaction does not occur heterogeneously on engine oil particles or on a large surface area of Teflon® material. Grassian (2002) observed HNO_3 heterogeneous uptake on mineral dust (alumina (Al_2O_3) and silica (SiO_2)) surfaces and heterogeneous HONO production reactions from NO_2 on soot or SiO_2 particles. Gustafsson et al. (2008) observed heterogeneous production of HONO on mineral dust (from the Gobi desert) from NO_2 and water. Because mineral dust aerosols have more polar surfaces when compared to the engine oil and Teflon® surfaces, they are hypothesized to be better candidates for heterogeneous conversion of HNO_3 to HONO. Two types of atmospherically abundant mineral dust materials were chosen for these experiments: carboxylate-doped SiO_2 and Al_2O_3.

Aqueous dispersions of size-calibrated 100-nm monodisperse spherical particles composed of either carboxylated-SiO_2 or pure Al_2O_3 (Corpuscular Inc., Cold Spring, NY) were used to generate aerosols for these experiments. These solutions were nebulized using an atomizer and subsequently dried using a diffusion-dryer and a heater (87.5 ± 1.5°C).

3. Results and Discussion

3.1 Base Case Results

Compared with the previous flow-tube study, the average base case f_{HONO} of 0.54 ± 0.09 ppb hr^{-1} (Table 1) agrees better with the observed 2006 Houston value of 0.6 ± 0.3 ppb hr^{-1} (Ziemba et al., 2010; Rutter et al., 2014). This could be attributed to improved measurement accuracy due to the refurbished MC/IC system. This observation also suggests that the reduction of HNO_3 to HONO by the reactive components of vehicular VOCs that were co-emitted with POA (Rutter et al., 2014) could be a dominant contributor to HONO formation events observed in Houston. The comparison here is qualitative because meteorology and vertical mixing conditions are highly variable in the atmosphere, and temperature ranged from 20.0 to 35.0°C during this field campaign (Lefer et al., 2010). Additionally, it is worth noting that experiments conducted using pure VOCs (toluene, isoprene, and hexadecane) in place of motor oil VOCs did not result in net HONO production, ruling out these VOCs as potential reactants. These experiments also rule out HONO artifacts from reactions other than (R3). In other words, despite the <10% HNO_3-to-HONO conversion efficiency we generally observe in the flow-tube system (Rutter et al., 2014), other nitrogen-containing compounds originating from HNO_3 reduction likely did not contribute to HONO production in this system.

Table 1 summarizes experimental data for each type of experiment. Mean values are reported for initial HNO_3 concentrations, f_{HONO}, and water vapor mixing ratios with N ≥ 3. All error bars and uncertainties reported here were propagated from measurement uncertainties, except those for initial HNO_3 concentrations with N ≥ 3, which are reported as standard deviations from the mean. The measurement uncertainties were larger than the standard deviations for f_{HONO} in most

experiment types, indicating high repeatability. Additional information on uncertainty is included in the Supporting Material.

The average HONO formation rates are not statistically different (within 1σ) when initial HNO_3 concentrations were ~400, 1 500, and 4 000 ppt, suggesting that the 200 - 300 ppt of reactive VOCs previously estimated by Rutter et al. (2014) (assuming a 1-to-1 stoichiometric ratio) remains the limiting factor. The lowest HNO_3 concentrations achieved in these experiments were ~400 ppt (by shutting off HNO_3 supply), which likely reflects the presence of HNO_3 in the air source or the desorption of HNO_3 from the supply tubing, since reactor walls were first rinsed with deionized water and baked under UV lights. A regression showing the weak relationship between f_{HONO} and HNO_3 mixing ratio is shown in Figure S1. Because HNO_3 concentrations above 400 ppt do not appear to significantly impact f_{HONO} , all seven HNO_3 experiments were grouped into one base case category (Table 1). This base case and the Houston 2006 average provide the benchmarks for comparison with other experiments (Figure 2).

3.2 Temperature

Although the mean f_{HONO} value for the combined base case experiments (T= 25°C) was lower than that for other temperatures, the f_{HONO} at 30.0°C and 35.0°C are not statistically different (within 1σ) than that of the base case. However, experiments at 20.0°C yielded significantly higher f_{HONO} (above 1σ). This could mean that the reaction rate increases at lower temperatures, but as mentioned previously this dependence may not follow an Arrhenius trend. This trend suggests the possibility that multiple reactions involving different reactive VOCs become more important at various temperatures. Sampling lines were insulated and heated such that HONO wall losses would be as small as possible, but it should be noted that any bias due to wall losses would likely decrease f_{HONO} at lower temperatures. The enhanced rate at lower temperatures could make the proposed reaction mechanism even more important at night.

3.3 NH_3

The presence of NH_3 had no observable impact on the reaction. Nitric acid concentrations were at ~ 3 500 ppt before NH_3 was introduced. After addition of NH_3, the system equilibrated at 118.0 ± 2.0 ppb NH_3 and 680 ± 52 ppt HNO_3. The formation of NH_4NO_3 and its subsequent partitioning into the solid phase is the likely cause for the observed consumption of HNO_3; any NH_4NO_3 particles formed would be filtered prior to entering the MC/IC. The f_{HONO} for these experiments also were similar to the base case, likely because HNO_3 was still in excess compared to the VOCs. This indicates that the neutralization reaction between NH_3 and HNO_3 does not directly interfere with the HONO formation reaction beyond the competition for HNO_3. Consistent with the experiments under varying HNO_3 levels, a lower f_{HONO} is not observed due to the decrease in HNO_3.

3.4 UV Light

When UV lights were turned on prior to experiments, a constant photolytic source of HONO from HNO_3 was observed, contributing to background HONO levels (net production of ~226 ppt or ~5.42

ppb hr^{-1}) in the reactor. Several sources could explain this HONO production, for example direct photolysis of HNO_3 sorbed on the reactor walls (Zhou et al., 2003) or from photolysis of nitrophenols (Bejan et al., 2006) that could be present in lubricating oil. We do not have the capability to isolate these sources, but they are not expected to bias f_{HONO} as defined here because formation rates are calculated using a step change in HONO when VOCs were removed during an experiment (Equation (1)). In other words, the HONO formation observed when VOCs were introduced under UV irradiation occurs above and beyond the background photolytic sources.

The observed average $f_{HONO,obs}$ under UV irradiation of 0.29 ± 0.17 ppb hr^{-1} was obtained using the change in HONO levels when VOCs were removed, similar to other experiments. However, according to a simplified mass balance (Equation (2)), the actual HONO production rate ($f_{HONO,UV}$) must correct for photolytic losses of HONO generated when VOCs were present to react with HNO_3:

$$f_{HONO,UV} = f_{HONO,obs} + J_{HONO}\,([HONO]_{UV+VOCs} - [HONO]_{UV}) \qquad \text{Equation (2)}$$

where J_{HONO} is the photolysis rate of HONO, and the term in brackets represents the difference in measured HONO mixing ratios with and without VOCs when the lights are illuminated. A spectroradiometer was not available to determine J_{HONO}. In Equation (2), an average J_{HONO} value of 1.75×10^{-3} s^{-1} was used. This value was derived from an average of measured ambient noon-time J_{HONO} (1.75×10^{-3} s^{-1} (Alicke et al., 2003) and 1.60×10^{-3} s^{-1}(Lee et al., 2013)) and J_{HONO} estimated using the method from Kraus and Hofzumahaus (1998) (1.90×10^{-3} s^{-1}) from NO_2 photolysis rates reported in an environmental chamber (Nakao et al., 2011) that utilized the same model of lights as this study. When corrected, the average $f_{HONO,\,UV}$ is 0.37 ± 0.17 ppb hr^{-1} (Table 1 and Figure 2). However, the J_{HONO} used here is likely much higher than the actual value from only four 40W UV lights, indicating that the $f_{HONO,\,UV}$ is likely an upper bound. To further test the uncertainty, the estimated value of J_{HONO} used was adjusted by factors of 0.5 and 2 to provide a range of 0.33 ± 0.17 to 0.44 ± 0.17 ppb hr^{-1} for the potential average $f_{HONO,UV}$ values.

Although $f_{HONO,\,UV}$ is within the uncertainty range of the base case f_{HONO}, it is likely that the reported $f_{HONO,\,UV}$ represents an upper bound and that the UV wavelengths studied here could directly interfere with the reduction reaction of HNO_3 to HONO. One explanation for this observation is that under UV irradiation, relevant organic compounds undergo oxidation by radicals formed in the reactor (Atkinson, 2000) or are photolyzed directly. This could alter the reactivity of the VOCs or reduce the total concentration of reactive VOCs available for reaction, hence slowing the overall reaction rate. This and additional tests (Support Material) support the hypothesis that VOCs are the limiting reactants in the reaction proposed here.

3.5 Mineral Dust Aerosol Surfaces

Neither carboxylated-SiO_2 nor Al_2O_3 particles (at concentrations of ~1600 #/cm^3) yielded significantly different f_{HONO} (within 1σ) than the base case (Figure 2). The slight decrease observed is counterintuitive if the surfaces are expected to enhance the reaction, indicating that the surfaces are potential minor loss sites for the reactive VOCs involved or for the HONO produced

(Romanias et al., 2012). This further affirms the probability that a surface is not required to convert HNO_3 to HONO via the proposed pathway.

4. Conclusions

Estimates of base case (25°C, ~20% RH) f_{HONO} derived from the reduction of HNO_3 by VOCs agree well with data from a 2006 field study in Houston (Ziemba et al., 2010) during which enhancements in HONO during morning rush hour were observed. The hypothesized reaction (R3) studied here could have been the main HONO source during the HONO formation events.

The HONO formation rate was relatively enhanced (~1.0 ppb hr^{-1}) at a lower temperature of ~20°C but statistically the same (~0.6 ppb hr^{-1}) in experiments at 25, 30 and 35°C. The assumption that multiple reactive components of the VOCs react with HNO_3 is supported by this observation, and the relative importance of each reactive species in the reaction may vary with temperature. The reaction rate is independent of initial HNO_3 concentration (> 400 ppt), suggesting that the concentration of reactive VOCs was the limiting factor. However, future work testing this reaction under HNO_3 concentrations < 400 ppt may provide insights into its relevance in cleaner environments. Ammonia gas consumed HNO_3 in the reactor (down to 680 ppt) but did not have a direct impact on the HONO formation reaction, providing further evidence that the rate is limited by the availability of VOCs in the experimental system. The $f_{HONO,UV}$ from (R3) was likely impeded by UV irradiation. Possible explanations for this observation include the photolysis/deactivation of the reactive VOCs involved in (R3) or the direct interference of UV light on (R3). Nonetheless, this observation must be confirmed by conducting a similar flow-tube study that focuses on constraining the reactive VOCs involved and quantifying HONO photolysis rates. The test of multiple atmospherically-relevant particle surfaces confirmed that the reaction proposed here does not require surfaces to proceed, despite the correlation that was observed in Houston in 2006 (Ziemba et al., 2010). Given the uncertainties, we observe substantial percentage changes in f_{HONO} between the base case and the 20°C and UV experiments, even when compared to the change when RH was varied from the base case to 1% or 50% in Rutter et al. (2014). The reduced sensitivity of f_{HONO} to other environmental variables tested here is also an important finding, especially in future modelling work aiming at incorporating this new HONO source to existing atmospheric models.

The HONO formation process studied here is likely homogeneous, but the results presented here do not rule out the possibility of a heterogeneous reaction pathway occurring in the atmosphere. Also, it is important to note that the net production of HONO observed in the UV experiments is in addition to production by background photolytic reactions that appear to be occurring on the wax-coated tube walls.

The gas-phase conversion of HNO_3 to HONO has significant air quality implications due to the "renoxification" of less reactive HNO_3 into more reactive HONO and should be tested in future modeling and field efforts. This pathway proceeds rapidly in the laboratory when compared with previously identified mechanisms (Table S3) and could potentially be an important source of HONO in the lower atmosphere (2^{nd} order rate constant ~1.0 x 10^{-7} ppt^{-1} s^{-1} estimated in Gall et al. (2015), in revision for *Atmospheric Environment*). Its role in HONO production aloft (synonymous

to the unknown gas-phase HONO source proposed by Li et al. (2014)) cannot yet be ruled out and should be evaluated in future work. In addition to their direct impact on O_3 formation and secondary organic aerosol formation, VOCs could also regulate the oxidative capacity of the atmosphere through the redox reaction studied here. These different processes have significant implications in terms of regional and global air quality. Hence, future experimental work focusing on the quantification of individual reactive components of the VOCs (e.g. utilizing mass spectrometry techniques coupled with proton transfer reaction or gas chromatography) that were involved in the reaction studied here (under varying environmental conditions) would allow detailed characterization of the HONO formation mechanism(s) and determination of reaction yields. Once the HONO formation reaction mechanism is well characterized, parameterizing the reaction would allow improvements in existing O_3 and PM prediction models.

Acknowledgements

We acknowledge financial support from the National Aeronautics and Space Administration (NASA Grant #NNX09AE26G S04). Ammonia measurements were supported by the Mid-InfraRed Technologies for Health and the Environment (MIRTHE) Center and National Science Foundation under grant No. EEC-0540832; Dan Campbell assisted in the ammonia experiments.

Supporting Material Available

Additional information and experiments (Text 1), uncertainty calculations (Text 2), least squares linear regression between f_{HONO} and initial HNO_3 concentration (Figure S1), the blend of engine oils used to generate the VOCs (Table S1), detailed measurement uncertainties and propagated errors in experiments (Table S2), estimated formation rates of previously proposed HONO sources (Table S3). This information is available free of charge via the Internet at http://www.atmospolres.com.

References

Alicke, B., Geyer, A., Hofzumahaus, A., Holland, F., Konrad, S., Pätz, H.W., Schäfer, J., Stutz, J., Volz-Thomas, A., Platt, U., 2003. Oh formation by hono photolysis during the berlioz experiment. *Journal of Geophysical Research: Atmospheres* 108, 8247.

Alicke, B., Platt, U., Stutz, J., 2002. Impact of nitrous acid photolysis on the total hydroxyl radical budget during the limitation of oxidant production/pianura padana produzione di ozono study in milan. *Journal of Geophysical Research: Atmospheres* 107, 8196.

Ammann, M., Kalberer, M., Jost, D.T., Tobler, L., Rossler, E., Piguet, D., Gaggeler, H.W., Baltensperger, U., 1998. Heterogeneous production of nitrous acid on soot in polluted air masses. *Nature* 395, 157-160.

Atkinson, R., 2000. Atmospheric chemistry of vocs and no_x. *Atmospheric Environment* 34, 2063-2101.

Bejan, I., Abd El Aal, Y., Barnes, I., Benter, T., Bohn, B., Wiesen, P., Kleffmann, J., 2006. The photolysis of ortho-nitrophenols: A new gas phase source of hono. *Physical Chemistry Chemical Physics* 8, 2028-2035.

Cape, J.N., Hargreaves, K.J., Storeton-West, R., Fowler, D., Colville, R.N., Choularton, T.W., Gallagher, M.W., 1992. Nitrite in orographic cloud as an indicator of nitrous acid in rural air. *Atmospheric Environment. Part A. General Topics* 26, 2301-2307.

University of California, Riverside, 1995. Environmental chamber studies of atmospheric reactivities of volatile organic compounds. Effects of varying chamber and light source. Final report, 95:AP:034F,

Carter, W.P.L., Seinfeld, J.H., 2012. Winter ozone formation and voc incremental reactivities in the upper green river basin of wyoming. *Atmospheric Environment* 50, 255-266.

Cazoir, D., Brigante, M., Ammar, R., D'Anna, B., George, C., 2014. Heterogeneous photochemistry of gaseous no2 on solid fluoranthene films: A source of gaseous nitrous acid (hono) in the urban environment. *Journal of Photochemistry and Photobiology a-Chemistry* 273, 23-28.

Cocker, D.R., Flagan, R.C., Seinfeld, J.H., 2001. State-of-the-art chamber facility for studying atmospheric aerosol chemistry. *Environmental Science & Technology* 35, 2594-2601.

Dibb, J.E., Arsenault, M., Peterson, M.C., Honrath, R.E., 2002. Fast nitrogen oxide photochemistry in summit, greenland snow. *Atmospheric Environment* 36, 2501-2511.

Dibb, J.E., Talbot, R.W., Bergin, M.H., 1994. Soluble acidic species in air and snow at summit, greenland. *Geophysical Research Letters* 21, 1627-1630.

Dibb, J.E., Talbot, R.W., Munger, J.W., Jacob, D.J., Fan, S.M., 1998. Air-snow exchange of hno_3 and no_y at summit, greenland. *Journal of Geophysical Research-Atmospheres* 103, 3475-3486.

Finlayson-Pitts, B.J., Pitts, J.N., 1997. Tropospheric air pollution: Ozone, airborne toxics, polycyclic aromatic hydrocarbons, and particles. *Science* 276, 1045-1052.

Gall, E.T., Dibb, J., Scheuer, E., Gong, L., Rutter, A.P., Karakurt Cevik, B., Kim, S., Lefer, B., Flynn, J., Griffin, R.J., 2015. Nitrous acid formation mechanisms in the outflow from a major urban area. *Atmospheric Environment (in revision)*.

Gong, L., Lewicki, R., Griffin, R.J., Flynn, J.H., Lefer, B.L., Tittel, F.K., 2011. Atmospheric ammonia measurements in houston, tx using an external-cavity quantum cascade laser-based sensor. *Atmospheric Chemistry and Physics* 11, 9721-9733.

Gong, L., Lewicki, R., Griffin, R.J., Tittel, F.K., Lonsdale, C.R., Stevens, R.G., Pierce, J.R., Malloy, Q.G.J., Travis, S.A., Bobmanuel, L.M., Lefer, B.L., Flynn, J.H., 2013. Role of atmospheric ammonia in particulate matter formation in houston during summertime. *Atmospheric Environment* 77, 893-900.

Grannas, A.M., Jones, A.E., Dibb, J., Ammann, M., Anastasio, C., Beine, H.J., Bergin, M., Bottenheim, J., Boxe, C.S., Carver, G., Chen, G., Crawford, J.H., Dominé, F., Frey, M.M., Guzmán, M.I., Heard, D.E., Helmig, D., Hoffmann, M.R., Honrath, R.E., Huey, L.G., Hutterli, M., Jacobi, H.W., Klán, P., Lefer, B., McConnell, J., Plane, J., Sander, R., Savarino, J., Shepson, P.B., Simpson, W.R., Sodeau, J.R., von Glasow, R., Weller, R., Wolff, E.W., Zhu, T., 2007. An overview of snow photochemistry: Evidence, mechanisms and impacts. *Atmospheric Chemistry and Physics* 7, 4329-4373.

Grassian, V.H., 2002. Chemical reactions of nitrogen oxides on the surface of oxide, carbonate, soot, and mineral dust particles: Implications for the chemical balance of the troposphere. *Journal of Physical Chemistry A* 106, 860-877.

Gustafsson, R.J., Kyriakou, G., Lambert, R.M., 2008. The molecular mechanism of tropospheric nitrous acid production on mineral dust surfaces. *ChemPhysChem* 9, 1390-1393.

Harris, G.W., Carter, W.P.L., Winer, A.M., Pitts, J.N., Platt, U., Perner, D., 1982. Observations of nitrous acid in the los angeles atmosphere and implications for predictions of ozone-precursor relationships. *Environmental Science & Technology* 16, 414-419.

Harrison, R.M., Peak, J.D., Collins, G.M., 1996. Tropospheric cycle of nitrous acid. *Journal of Geophysical Research: Atmospheres* 101, 14429-14439.

Indarto, A., 2012. Heterogeneous reactions of hono formation from no_2 and hno_3: A review. *Research on Chemical Intermediates* 38, 1029-1041.

Kalberer, M., Ammann, M., Arens, F., Gaggeler, H.W., Baltensperger, U., 1999. Heterogeneous formation of nitrous acid (hono) on soot aerosol particles. *Journal of Geophysical Research-Atmospheres* 104, 13825-13832.

Kanakidou, M., Seinfeld, J.H., Pandis, S.N., Barnes, I., Dentener, F.J., Facchini, M.C., Van Dingenen, R., Ervens, B., Nenes, A., Nielsen, C.J., Swietlicki, E., Putaud, J.P., Balkanski, Y., Fuzzi, S., Horth, J., Moortgat, G.K., Winterhalter, R., Myhre, C.E.L., Tsigaridis, K., Vignati, E., Stephanou, E.G., Wilson, J., 2005. Organic aerosol and global climate modelling: A review. *Atmospheric Chemistry and Physics* 5, 1053-1123.

Kirchstetter, T.W., Harley, R.A., Littlejohn, D., 1996. Measurement of nitrous acid in motor vehicle exhaust. *Environmental Science & Technology* 30, 2843-2849.

Kleffmann, J., 2007. Daytime sources of nitrous acid (hono) in the atmospheric boundary layer. *ChemPhysChem* 8, 1137-1144.

Kraus, A., Hofzumahaus, A., 1998. Field measurements of atmospheric photolysis frequencies for o-3, no2, hcho, ch3cho, h2o2, and hono by uv spectroradiometry. *Journal of Atmospheric Chemistry* 31, 161-180.

Lee, B.H., Wood, E.C., Herndon, S.C., Lefer, B.L., Luke, W.T., Brune, W.H., Nelson, D.D., Zahniser, M.S., Munger, J.W., 2013. Urban measurements of atmospheric nitrous acid: A caveat on the interpretation of the hono photostationary state. *Journal of Geophysical Research: Atmospheres* 118, 2013JD020341.

1 Lefer, B., Rappenglück, B., Flynn, J., Haman, C., 2010. Photochemical and meteorological
2 relationships during the texas-ii radical and aerosol measurement project (tramp). *Atmospheric*
3 *Environment* 44, 4005-4013.

4 Lei, W., Zhang, R., Tie, X., Hess, P., 2004. Chemical characterization of ozone formation in the
5 houston-galveston area: A chemical transport model study. *Journal of Geophysical Research:*
6 *Atmospheres* 109, D12301.

7 Li, X., Rohrer, F., Hofzumahaus, A., Brauers, T., Haseler, R., Bohn, B., Broch, S., Fuchs, H., Gomm, S.,
8 Holland, F., Jager, J., Kaiser, J., Keutsch, F.N., Lohse, I., Lu, K.D., Tillmann, R., Wegener, R., Wolfe,
9 G.M., Mentel, T.F., Kiendler-Scharr, A., Wahner, A., 2014. Missing gas-phase source of hono
10 inferred from zeppelin measurements in the troposphere. *Science* 344, 292-296.

11 Liu, Z., Wang, Y., Costabile, F., Amoroso, A., Zhao, C., Huey, L.G., Stickel, R., Liao, J., Zhu, T., 2014.
12 Evidence of aerosols as a media for rapid daytime hono production over china. *Environmental*
13 *Science & Technology* 48, 14386-14391.

14 Nakao, S., Shrivastava, M., Nguyen, A., Jung, H.J., Cocker, D., 2011. Interpretation of secondary
15 organic aerosol formation from diesel exhaust photooxidation in an environmental chamber.
16 *Aerosol Science and Technology* 45, 9.

17 Reisinger, A.R., 2000. Observations of hno_2 in the polluted winter atmosphere: Possible
18 heterogeneous production on aerosols. *Atmospheric Environment* 34, 3865-3874.

Rivera-Figueroa, A.M., Sumner, A.L., Finlayson-Pitts, B.J., 2003. Laboratory studies of potential mechanisms of renoxification of tropospheric nitric acid. *Environmental Science & Technology* 37, 548-554.

Romanias, M.N., El Zein, A., Bedjanian, Y., 2012. Reactive uptake of hono on aluminium oxide surface. *Journal of Photochemistry and Photobiology a-Chemistry* 250, 50-57.

Rutter, A.P., Malloy, Q.G.J., Leong, Y.J., Gutierrez, C.V., Calzada, M., Scheuer, E., Dibb, J.E., Griffin, R.J., 2014. The reduction of hno_3 by volatile organic compounds emitted by motor vehicles. *Atmospheric Environment* 87, 200-206.

Spataro, F., Ianniello, A., 2014. Sources of atmospheric nitrous acid: State of the science, current research needs, and future prospects. *Journal of the Air & Waste Management Association* 64, 1232-1250.

Stutz, J., Kim, E.S., Platt, U., Bruno, P., Perrino, C., Febo, A., 2000. Uv-visible absorption cross sections of nitrous acid. *Journal of Geophysical Research-Atmospheres* 105, 14585-14592.

Stutz, J., Oh, H.-J., Whitlow, S.I., Anderson, C., Dibb, J.E., Flynn, J.H., Rappenglück, B., Lefer, B., 2010. Simultaneous doas and mist-chamber ic measurements of hono in houston, tx. *Atmospheric Environment* 44, 4090-4098.

Talbot, R.W., Vijgen, A.S., Harriss, R.C., 1990. Measuring tropospheric hno_3 - problems and prospects for nylon filter and mist chamber techniques. *Journal of Geophysical Research-Atmospheres* 95, 7553-7561.

VandenBoer, T.C., Young, C.J., Talukdar, R.K., Markovic, M.Z., Brown, S.S., Roberts, J.M., Murphy, J.G., 2015. Nocturnal loss and daytime source of nitrous acid through reactive uptake and displacement. *Nature Geosci* 8, 55-60.

Wong, K.W., Oh, H.J., Lefer, B.L., Rappenglueck, B., Stutz, J., 2011. Vertical profiles of nitrous acid in the nocturnal urban atmosphere of houston, tx. *Atmospheric Chemistry and Physics* 11, 3595-3609.

Worton, D.R., Isaacman, G., Gentner, D.R., Dallmann, T.R., Chan, A.W.H., Ruehl, C., Kirchstetter, T.W., Wilson, K.R., Harley, R.A., Goldstein, A.H., 2014. Lubricating oil dominates primary organic aerosol emissions from motor vehicles. *Environmental Science & Technology* 48, 3698-3706.

Zhou, X.L., Gao, H.L., He, Y., Huang, G., Bertman, S.B., Civerolo, K., Schwab, J., 2003. Nitric acid photolysis on surfaces in low-nox environments: Significant atmospheric implications. *Geophysical Research Letters* 30, 2217.

Zhou, X.L., He, Y., Huang, G., Thornberry, T.D., Carroll, M.A., Bertman, S.B., 2002. Photochemical production of nitrous acid on glass sample manifold surface. *Geophysical Research Letters* 29, 4.

Zhou, X.L., Zhang, N., TerAvest, M., Tang, D., Hou, J., Bertman, S., Alaghmand, M., Shepson, P.B., Carroll, M.A., Griffith, S., Dusanter, S., Stevens, P.S., 2011. Nitric acid photolysis on forest canopy surface as a source for tropospheric nitrous acid. *Nature Geoscience* 4, 440-443.

Ziemba, L.D., Dibb, J.E., Griffin, R.J., Anderson, C.H., Whitlow, S.I., Lefer, B.L., Rappenglück, B., Flynn, J., 2010. Heterogeneous conversion of nitric acid to nitrous acid on the surface of primary organic aerosol in an urban atmosphere. *Atmospheric Environment* 44, 4081-4089.

1

2

Figure and Table Captions

Figure 1. Flow diagram of the flow-tube system and instrumentation. Dashed lines represent heated lines for the flow of low-volatility gases (CPC = condensation particle counter).

Figure 2. Average HONO formation rates (with error bars) for each experimental category and comparison to the base case (25.0°C and ~20.0% RH without the addition of NH_3, dust particles, or UV irradiation) and field results from Ziemba et al. (2010). HighN, MedN, and LowN represent experiments with high HNO_3, medium HNO_3, and low HNO_3, respectively, and are combined to generate the average base case output. The average HONO formation rate for UV experiments was corrected for photolytic HONO losses (see Section 3.4).

Table 1. Summary of experimental conditions and average HONO formation rates.

Figures

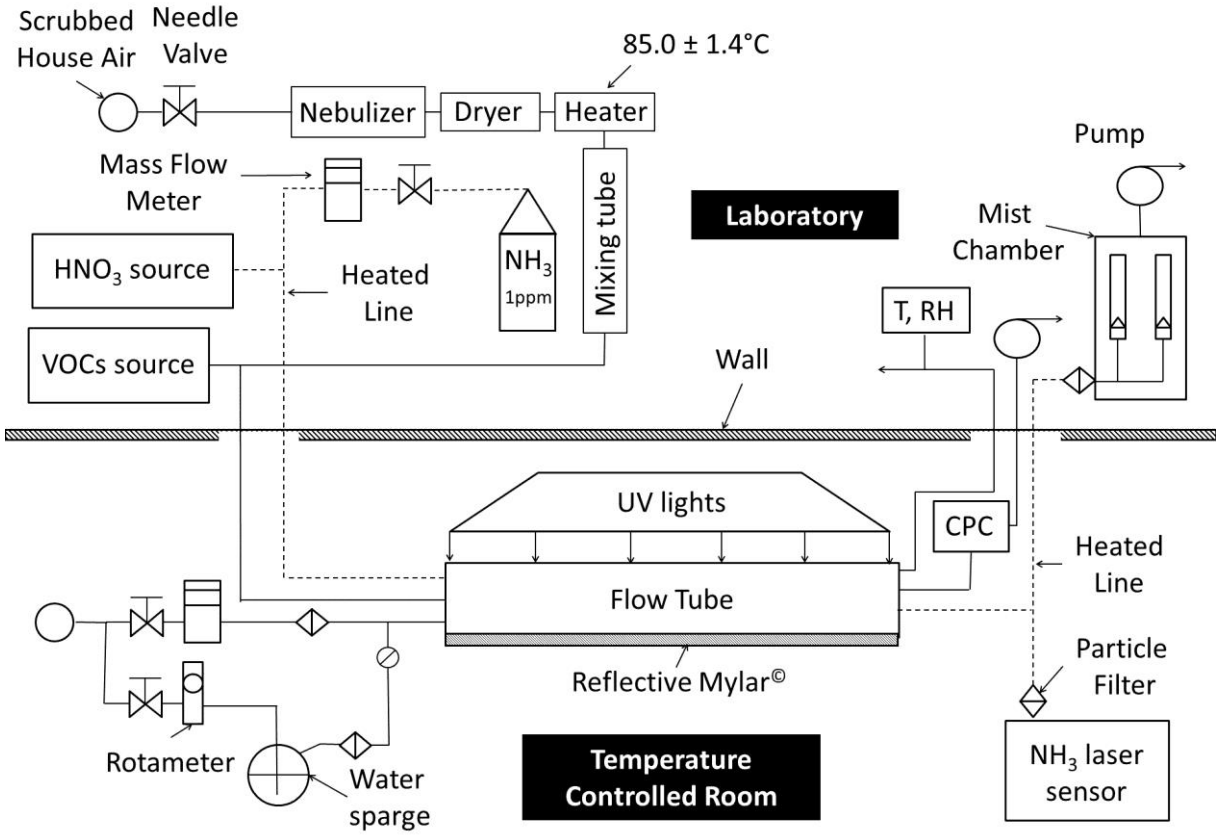

Figure 1.

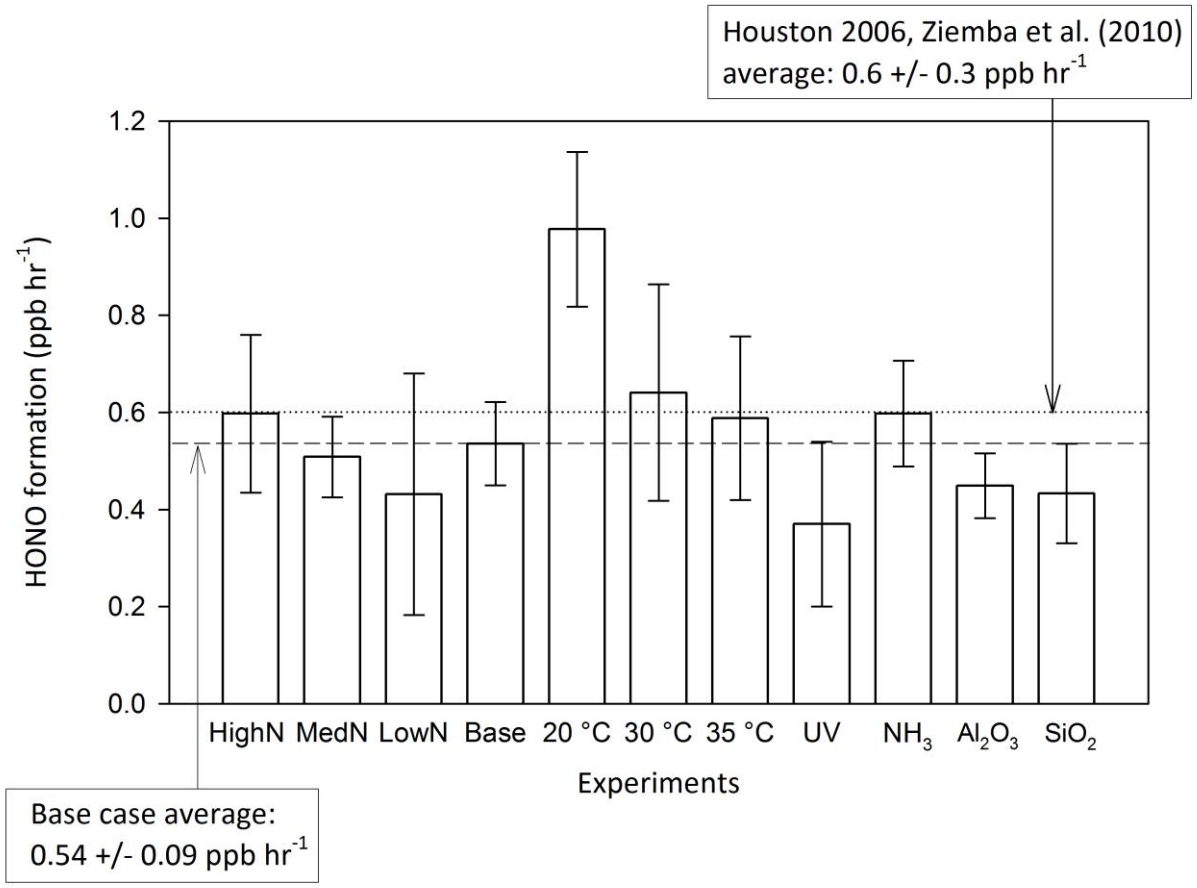
Houston 2006, Ziemba et al. (2010)
average: 0.6 +/- 0.3 ppb hr-1
HONO formation (ppb hr-1)
1.2
1.0
0.8
0.6
0.4
0.2
0.0
HighN
MedN
LowN
Base
20 °C
30 °C
35 °C
UV
NH3
Al2O3
SiO2
Experiments
Base case average:
0.54 +/- 0.09 ppb hr-1

Figure 2.

Tables

Table 1.

Experiment	Initial HNO_3 (ppt)	Unc/stdev (ppt)	N[a]	f_{HONO} (ppb/hr)	Unc /stdev (ppb/hr)	Water Vapor Mixing ratio (%)	Notes
Base case, High HNO_3	3 980	936	3	0.60	0.16	0.67	T = 25.0°C
Base case, Medium HNO_3	1 522	159	3	0.51	0.08	0.63	T = 25.0°C
Base case, Low HNO_3	399	53	1	0.43	0.25	0.58	T = 25.0°C
Base case, all HNO_3 levels	2 415	1 613	7	0.54	0.09	0.64	T = 25.0°C
T = 20.0 °C	2 763	52	3	0.98	0.16	0.86	
T = 30.0 °C	4 344	361	4	0.64	0.22	0.73	
T = 35.0 °C	3 755	474	4	0.59	0.17	0.98	
UV Irradiation	3 405	451	3	0.37	0.17	0.59	Corrected for UV losses
Ammonia	680	52	3	0.60	0.11	0.73	NH_3 = 118.0 ± 2.0 ppb
Alumina aerosol	3 356	346	3	0.45	0.07	0.61	Average count = 1600 #/cm^3
Silica-COOH aerosol	3 443	85	3	0.43	0.10	0.60	Average count = 1600 #/cm^3

[a] N = number of experiments conducted

Supporting Material

Impact of Environmental Variables on the Reduction of Nitric Acid by Proxies for Volatile Organic Compounds Emitted by Motor Vehicles

Leong Y. J.[1]*; Rutter, A. P.[1,2]; Wong, H. Y.[1,3]; Gutierrez, C. V.[1]; Junaid, M.[1]; Scheuer, E.[4]; Gong, L.[1,5] ; Lewicki, R.[6,7]; Dibb, J. E.[4]; Tittel, F. K.[6]; Griffin, R. J.[1]

[1] Rice University, Civil and Environmental Engineering, 6100 Main Street MS-519, Houston, TX 77005

[2] (Current) Collaborative Sciences Division, S.C. Johnson, Inc., 1525 Howe St., Racine, WI 53403

[3] (Current) Behn Meyer Group Malaysia, 5, Jalan TP2 Sime UEP Industrial Park, Subang Jaya, Selangor, 47600, Malaysia

[4] University of New Hampshire, Earth Systems Research Center, Morse Hall, Durham, NH 03824

[5] (Current) Monitoring and Laboratory Division, California Air Resources Board, 1900 14th Street, Sacramento, CA 95811

[6] Department of Electrical and Computer Engineering, Rice University, 6100 Main Street, MS 366, Houston, TX 77005

[7] (Current) Sentinel Photonics, 45 Wall Street, Princeton, NJ 08540

*Corresponding author: Yu Jun Leong, Email: yu.jun.leong@gmail.com. Phone: (713) 348-3036. Fax: (713) 348-5268.

Table of Contents

1. Additional information and experiments

The reader is referred to section 2.4 of our previous manuscript (Rutter et al., 2014) for a detailed discussion of the choice of engine oil VOCs used as proxies for vehicular emissions. Background levels of HONO (~30 ppt) and HNO_3 (~400 ppt) in the reactor were achieved upon rinsing the system with water and baking with UV lights for ~8 hours.

Experiments conducted using several pure organic compounds (such as toluene, isoprene, and hexadecane) instead of engine oil VOCs did not result in HONO production.

Three experiments were conducted at T = 20 °C and by diluting the source of VOCs with clean air prior to injection to the flow-tube reactor (other conditions were identical to the T = 20 °C experiments). The diluted concentration of reactive VOCs in the reactor was estimated based on mass balance to be ~55% of the nominal concentration used. The dilution of VOCs resulted in f_{HONO}

of 0.72 ± 0.22 ppb hr^{-1}, which is lower when compared with f_{HONO} of 0.96 ± 0.18 ppb hr^{-1} for the nominal T= 20°C experiments (Table 1). This comparison provides supporting evidence that the concentration of VOCs was the limiting factor for the reaction discussed here. However, these experiments were not used in direct comparison with the other experimental categories because two variables (temperature and concentration of VOCs) were changed simultaneously.

Tests were also conducted to rule out heterogeneous reactions in the flow tube reactor, by measuring f_{HONO} under varying residence times while keeping other parameters constant. The f_{HONO} for different residence times were statistically similar, which lends support to our case that HONO formation occurred predominantly in the gas phase.

2. Uncertainty calculations

Weekly calibrations for the mist chamber/ion-chromatography (MC/IC) were conducted to minimize systematic errors in HONO mixing ratio measurements ([HONO] in ppt). The overall measurement uncertainties in $[HONO]_t$ and $[HONO]_0$ in Equation (1) were estimated from the standard deviation of 1-hour averages of steady-state [HONO] (immediately prior to and after the removal of VOCs). These uncertainties were propagated to the f_{HONO} "Unc" values for individual experiments as shown in Table S2. When calculating the mean f_{HONO} value for each experimental category, the individual uncertainties are again propagated to give an estimate of the uncertainty in the averaged f_{HONO} value ("Prop"). These propagated measurement uncertainties are larger than the spread in f_{HONO} values for each category (standard deviation of the average, "Stdev"), indicating good repeatability. The same procedures were used to calculate initial [HNO_3] and [HONO] values (also shown in Table S2). The larger of either the 'Stdev.' or 'Prop.' values for initial [HNO_3] or f_{HONO} were used to represent their respective uncertainty ranges in Table 1 and Figure 2 in the main text.

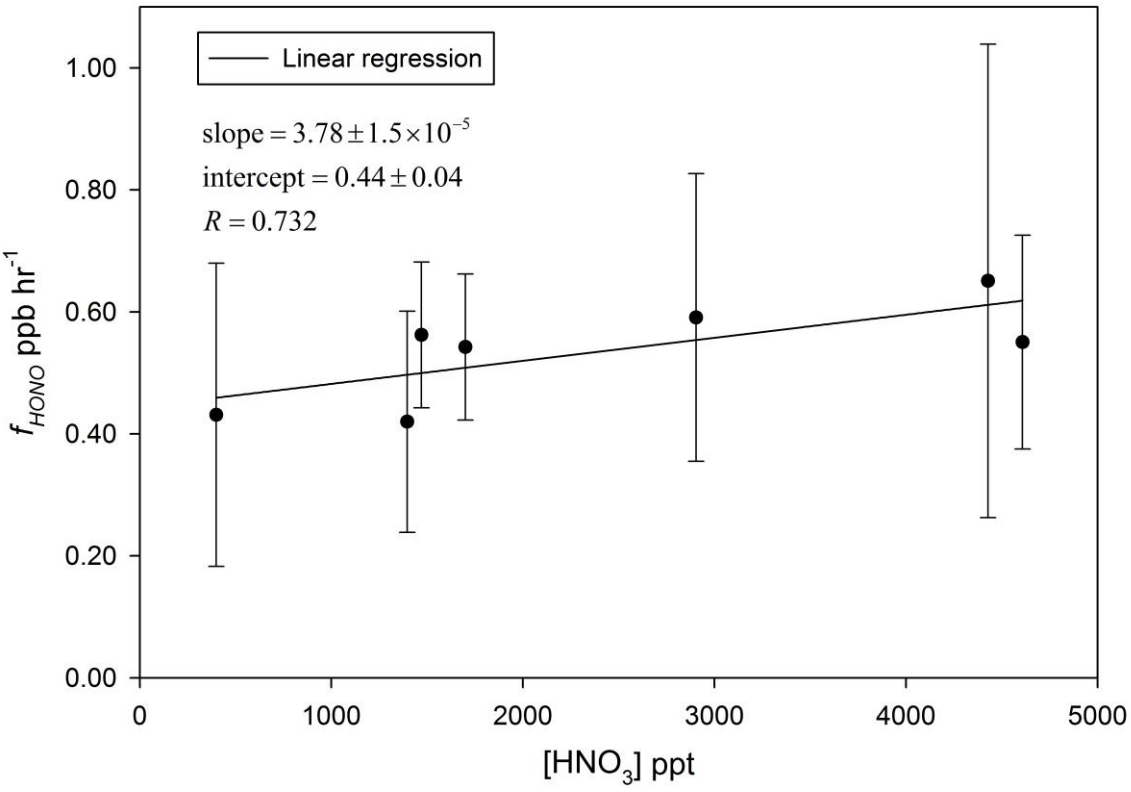

Figure S1. Least squares linear regression between f_{HONO} and initial HNO_3 concentration from seven experiments conducted at varying HNO_3 concentrations. The slope and intercept are reported with standard error estimated from the linear regression and have units of ppb hr^{-1} ppt^{-1} and ppb hr^{-1} respectively.

1

Table S1. The blend of engine oils used to generate the VOCs in this study (adapted from Rutter et al. (2014))

Name	Grade	Intended Engine Type	Volume (ml)
Castrol GTX	5W-30	Gasoline	25
Castrol GTX	10W-30	Gasoline	25
Mobil 1 High Mileage	5W-30	Gasoline	25
Mobil 1 High Mileage	10W-30	Gasoline	25
Mobil 1 Extended Performance	5W-20	Gasoline	25
Valvoline Premium Conventional	5W-30	Gasoline	25
Valvoline Premium Conventional	10W-30	Gasoline	25
Quaker State Advanced Durability	5W-30	Gasoline	25
Quaker State Advanced Durability	10W-30	Gasoline	25
Pennzoil Active	5W-30	Gasoline	25
Pennzoil Active	10W-30	Gasoline	25
Pennzoil Active	5W-20	Gasoline	25
Castrol GTX Diesel	15W-40	Diesel	115

2

3

1

Table S2. Detailed measurement uncertainties and propagated errors in experiments. 'Unc' values for individual experiments represent errors propagated from measurement uncertainties. Rows denoted with 'Stdev.' refer to standard deviations of the calculated average values; rows denoted with 'Prop.' refer to the propagated errors of the average.

Expt No.	Category	Initial $[HNO_3]$ (ppt)	Unc type	Unc (ppt)	Initial [HONO] (ppt)	Unc (ppt)	f_{HONO} (ppb hr^{-1})	Unc (ppb hr^{-1})
1	Base case, High HNO_3	4608		77	63.7	1.5	0.55	0.18
2	Base case, High HNO_3	4428		30	67.4	0.8	0.65	0.39
3	Base case, High HNO_3	2904		29	70.5	1.9	0.59	0.24
Avg	Base case, High HNO_3	3980	Stdev.	936	67.2	3.4	0.60	0.05
			Prop.	29		0.8		0.16
4	Base case, Med HNO_3	1471		11	40.6	0.7	0.56	0.12
5	Base case, Med HNO_3	1700		26	39.8	1.1	0.54	0.12
6	Base case, Med HNO_3	1395		8	43.9	1.0	0.42	0.18
Avg	Base case, Med HNO_3	1522	Stdev.	159	41.4	2.2	0.51	0.08
			Prop.	10		0.5		0.08
7	Base case, Low HNO_3	399		53	47.2	1.9	0.43	0.25
Avg	Base case, all HNO3	2415	Stdev.	1613	53.3	13.4	0.54	0.08
			Prop.	15		1.2		0.09
8	T = 20.0 °C	2704		35	45.2	0.9	1.14	0.20
9	T = 20.0 °C	2740		27	46.2	1.7	0.93	0.23
10	T = 20.0 °C	2785		79	51.1	1.1	0.93	0.22
11	T = 20.0 °C	2823		55	58.5	2.1	0.91	0.30
Avg	T = 20.0 °C	2763	Stdev.	52	50.3	6.1	0.98	0.11
			Prop.	35		1.0		0.16
12	T = 30.0 °C	4741		22	75.4	4.2	0.78	0.41
13	T = 30.0 °C	4505		24	95.2	3.5	0.36	0.35
14	T = 30.0 °C	4227		27	75.5	1.9	0.78	0.30
15	T = 30.0 °C	3904		20	76.8	2.5	0.65	0.27
Avg	T = 30.0 °C	4344	Stdev.	361	80.7	9.7	0.64	0.20
			Prop.	16		2.1		0.22
16	T = 35.0 °C	4389		21	104.3	3.0	0.59	0.27
17	T = 35.0 °C	3838		24	71.0	2.6	0.53	0.37
18	T = 35.0 °C	3448		25	69.1	1.5	0.77	0.17
19	T = 35.0 °C	3343		42	76.2	1.1	0.47	0.13
Avg	T = 35.0 °C	3755	Stdev.	474	80.2	16.4	0.59	0.13
			Prop.	19		1.5		0.17
20	UV Irradiation	2886		71	315.1	2.4	0.30	0.24
21	UV Irradiation	3704		59	263.4	2.2	0.33	0.29
22	UV Irradiation	3625		21	251.1	3.7	0.24	0.33
Avg	UV Irradiation (uncorrected)	3405	Stdev.	451	276.5	34.0	0.29	0.04
			Prop.	32		1.6		0.17
	UV Irradiation		Prop.				0.37	0.17

(corrected, Eq. (2))

Table S1 (continued)

Expt No.	Category	Initial $[HNO_3]$ (ppt)	Unc type	Unc (ppt)	Initial [HONO] (ppt)	Unc (ppt)	f_{HONO} (ppb hr^{-1})	Unc (ppb hr^{-1})
23	Ammonia	3370		53	95.4	1.6	0.58	0.17
24	Ammonia	3717		71	96.1	1.4	0.61	0.20
25	Ammonia	3909		66	97.9	1.1	0.60	0.20
Avg	Ammonia	3666	Stdev.	273	96.5	1.3	0.60	0.01
			Prop.	37		0.8		0.11
26	Alumina aerosol	3565		29	88.5	0.5	0.40	0.14
27	Alumina aerosol	2956		116	92.7	0.8	0.57	0.11
28	Alumina aerosol	3546		46	81.6	0.6	0.38	0.08
Avg	Alumina aerosol	3356	Stdev.	346	87.6	5.6	0.45	0.10
			Prop.	43		0.4		0.07
29	Silica aerosol	3541		24	90.0	0.4	0.36	0.08
30	Silica aerosol	3393		15	91.3	1.2	0.38	0.27
31	Silica aerosol	3394		18	89.6	0.5	0.56	0.13
Avg	Silica aerosol	3443	Stdev.	85	90.3	0.9	0.43	0.11
			Prop.	11		0.5		0.10

1

2

1

Table S3. Estimated rates of previously identified HONO formation mechanisms using observed or typical ambient parameters. Parameters used in the source strength calculations are included below.

Source rank	HONO source mechanism	Estimated source strength (ppb hr^{-1})	Input parameters	Daytime/ Nighttime	Reference
1	Gas-phase source that scales with J_{HONO}	0.69	S_{HONO}, J_{HONO}	Day	*Li et al. (2014)*
2	Homogeneous source (HNO_3 and VOCs)	0.54	-	Day/Night	*This study*
3	Photolysis of surface-adsorbed HNO_3 (scaled by [HNO_3])	0.54	P_{HNO3}, [HNO_3]	Day	*Zhou et al. (2003)*
4	Reaction between OH and NO	0.33	k_{OH-NO}, [OH], [NO]	Day	*Atkinson et al. (2004)*
5	NO_2 surface production	0.004	γ_{NO2}, h, [NO_2]	Day/Night	*VandenBoer et al. (2013)*
6	NO_2 hydrolysis on aerosol surface	0.0002	k_{NO2}, S/V, [NO_2]	Day/Night	*Kurtenbach et al. (2001)*

2

Parameter	Symbol	Units	Value	Reference
HONO production rate	S_{HONO}	ppt s h^{-1} × J_{HONO}	4.05E+05	*Li et al. (2014)*
Ambient noon-time HONO photolysis rate	J_{HONO}	s^{-1}	1.70E-03	(Alicke et al. (2003); Lee et al. (2013))
HONO production (700 ppt HNO_3)	P_{HNO3}	ppb hr^{-1}	1.50E-01	*Zhou et al. (2003)*
Rate constant	k_{OH-NO}	[N_2] cm^3 $molecule^{-1}$ s^{-1}	7.52E-31	*Atkinson et al. (2004)*
NO_2 uptake coefficient	γ_{NO2}	-	2.00E-06	*VandenBoer et al. (2013)*
Rate constant	k_{NO2}	(S/V) min^{-1} m^{-1}	3.00E-03	*Kurtenbach et al. (2001)*
Experimental nitric acid levels	[HNO_3]	ppt	2500	*This study*
12-hr daytime hydroxyl radical	[OH]	ppt	0.08	*Atkinson (2000)*
Assumed daytime nitrogen oxide	[NO]	ppb	2.5	-
Assumed daytime nitrogen dioxide	[NO_2]	ppb	5	-
Daytime boundary layer height, Houston	h	m	400	*Banta et al. (2005)*
Median aerosol surface area, Houston	S/V	mm^2 cm^{-3}	232	*(Ziemba et al. (2010))*

3

References

Alicke, B., Geyer, A., Hofzumahaus, A., Holland, F., Konrad, S., Pätz, H.W., Schäfer, J., Stutz, J., Volz-Thomas, A., Platt, U., 2003. Oh formation by hono photolysis during the berlioz experiment. *Journal of Geophysical Research: Atmospheres* 108, 8247.

Atkinson, R., 2000. Atmospheric chemistry of vocs and no_x. *Atmospheric Environment* 34, 2063-2101.

Atkinson, R., Baulch, D.L., Cox, R.A., Crowley, J.N., Hampson, R.F., Hynes, R.G., Jenkin, M.E., Rossi, M.J., Troe, J., 2004. Evaluated kinetic and photochemical data for atmospheric chemistry: Volume i - gas phase reactions of o-x, hox, nox and sox species. *Atmospheric Chemistry and Physics* 4, 1461-1738.

Banta, R.M., Senff, C.J., Nielsen-Gammon, J., Darby, L.S., Ryerson, T.B., Alvarez, R.J., Sandberg, S.R., Williams, E.J., Trainer, M., 2005. A bad air day in houston. *Bulletin of the American Meteorological Society* 86, 657-+.

Kurtenbach, R., Becker, K.H., Gomes, J.A.G., Kleffmann, J., Lorzer, J.C., Spittler, M., Wiesen, P., Ackermann, R., Geyer, A., Platt, U., 2001. Investigations of emissions and heterogeneous formation of hono in a road traffic tunnel. *Atmospheric Environment* 35, 3385-3394.

Lee, B.H., Wood, E.C., Herndon, S.C., Lefer, B.L., Luke, W.T., Brune, W.H., Nelson, D.D., Zahniser, M.S., Munger, J.W., 2013. Urban measurements of atmospheric nitrous acid: A caveat on the interpretation of the hono photostationary state. *Journal of Geophysical Research: Atmospheres* 118, 2013JD020341.

Li, X., Rohrer, F., Hofzumahaus, A., Brauers, T., Haseler, R., Bohn, B., Broch, S., Fuchs, H., Gomm, S., Holland, F., Jager, J., Kaiser, J., Keutsch, F.N., Lohse, I., Lu, K.D., Tillmann, R., Wegener, R., Wolfe, G.M., Mentel, T.F., Kiendler-Scharr, A., Wahner, A., 2014. Missing gas-phase source of hono inferred from zeppelin measurements in the troposphere. *Science* 344, 292-296.

Rutter, A.P., Malloy, Q.G.J., Leong, Y.J., Gutierrez, C.V., Calzada, M., Scheuer, E., Dibb, J.E., Griffin, R.J., 2014. The reduction of hno_3 by volatile organic compounds emitted by motor vehicles. *Atmospheric Environment* 87, 200-206.

VandenBoer, T.C., Brown, S.S., Murphy, J.G., Keene, W.C., Young, C.J., Pszenny, A.A.P., Kim, S., Warneke, C., de Gouw, J.A., Maben, J.R., Wagner, N.L., Riedel, T.P., Thornton, J.A., Wolfe, D.E., Dube, W.P., Ozturk, F., Brock, C.A., Grossberg, N., Lefer, B., Lerner, B., Middlebrook, A.M., Roberts, J.M., 2013. Understanding the role of the ground surface in hono vertical structure: High resolution vertical profiles during nachtt-11. *Journal of Geophysical Research-Atmospheres* 118, 10155-10171.

Zhou, X.L., Gao, H.L., He, Y., Huang, G., Bertman, S.B., Civerolo, K., Schwab, J., 2003. Nitric acid photolysis on surfaces in low-nox environments: Significant atmospheric implications. *Geophysical Research Letters* 30, 2217.

Ziemba, L.D., Dibb, J.E., Griffin, R.J., Anderson, C.H., Whitlow, S.I., Lefer, B.L., Rappenglück, B., Flynn, J., 2010. Heterogeneous conversion of nitric acid to nitrous acid on the surface of primary organic aerosol in an urban atmosphere. *Atmospheric Environment* 44, 4081-4089.